Numerical solution for a fluid-active structure interaction

Andrea Bucchi[1]*, Jing Tang Xing[2], and Paolo Gaudenzi[3]
[1] Dipartimento di Ingegneria Aerospaziale e Astronautica, University of Rome "La Sapienza", Italy
andrea.bucchi@uniroma1.it
[2] The School of Engineering Sciences, University of Southampton, United Kingdom
[3] Dipartimento di Ingegneria Aerospaziale e Astronautica, University of Rome "La Sapienza", Italy

ABSTRACT

Modelling of multiphysics problems is essential in many engineering fields, such as aerospace, automotive, bio-medical, civil and naval engineering: current trends are to develop and solve physic models, more accurate and representative of real complex systems.
In this paper we present a numerical solution for a fluid-active structure interaction and our procedure is tested on two simple problems in a bi-dimensional domain; procedure can be extended to three dimensional domains and used to study industrial applications.
First problem examined is the mass adduction of an incompressible fluid flow in a rectangular bi-dimensional domain: the walls are fixed except for the top wall that is like a double clamped beam. Beam is bended under the fluid pressure and bending deformations are revealed from piezoelectric patches bounded on the beam surface. Beam is modelled with solid bi-dimensional element under plain-strain hypothesis.
Second problem studied is the inflation of a rectangular section: injection of an incompressible flow, at low speed, is used to inflate a thin solid structure and piezoelectric patches are used as sensors to monitor the process. Fluid domain has all moving boundaries (interface with structure) except for the inlet zone that is fixed in space; during inflation the structure is deformed, stretched and wrinkled and piezoelectric patches transform these mechanical inputs in an electrical output (electric potential) that can be used as a structural health monitoring.
A mixed finite element formulation is used to solve the non linear incompressible, viscous and time dependent two dimensional fluid flow and a classical finite element displacement formulation, for linear elasticity, is used to solve an active structure made of solid with piezoelectric material.
To avoid ill-shaped elements and achieve a better solution, an updating mesh algorithm is used near the interface zone during time integration.
Numerical results are then presented and discussed; a comparison with theoretical model or results available in literature is presented where possible.

Keywords: finite element, incompressible fluid, piezoelectric, active structure, fluid structure interaction.

1. INTRODUCTION

A numerical procedure based on finite element method is presented to solve multyphisics problems involving three different physic fields: fluid structure interaction among incompressible viscous fluid flow, solid structure and piezoelectric material.
Viscous fluid gives forces to the structure due to normal stresses (pressure) and shear stresses (velocity); these forces deform the structure and the deformation is revealed and transformed by piezoelectric material (sensor), via a charge amplifier, in an electric output (voltage).
The finite element method has been selected in the analysis, for its versatility in manage complex

geometry involved in problem of practical interest.
A well established literature is now available for problem involving fluid structure interaction between incompressible fluid flow and linear (or nonlinear) structure [1,2] using finite element technique; also advanced finite element model are used to simulate piezoelectric material embedded in solid structure, for example in [3] a laminated shell with active layers made by piezoelectric is developed using a finite element mixed formulation; but no paper about an interaction between fluid and structure with piezoelectric material is available in scientific literature.
In our opinion it is important to establish a suitable numerical procedure to analyse and predict the behaviour of complex systems arising in many engineering field.
Incompressible and viscous fluid flow represents an important area in theoretical and computational fluid dynamics, with a fundamental role in applied science [4]; for example it is incompressible the air-flow around automobiles or low-speed airplanes, water-flow around a ship or inside a pipe, or the blood flow into a vein.
Physically, incompressible flow has a low Mach number (typically Ma <0.3).
Mathematically, incompressibility condition enforces a divergence free velocity field that is a strong and strict condition to verify in computation.
Fluid is coupled in a two-ways with a solid structure hosting piezoelectric material to enhance passive structure with new features and capabilities; this kind of structure is an active structure.
Piezoelectric material exhibits a two-ways coupling between mechanical field and electric field [5].
Direct piezoelectric effect transforms mechanical force applied to the material, in electric voltage hence piezoelectric material is used as sensor; typical applications are strain gages, pressure transducers and accelerometers [5]. An advanced use of piezoelectric as sensor is in structural health monitoring [6].
Converse piezoelectric effect transforms an electrical input, voltage, in a mechanical output such as structure deformation, hence piezoelectric material is used as actuator. An advanced use of piezoelectric as actuator is in microelectromechanical systems (MEMS) [7] or in structural shape morphing (e.g. inflatable wing) [8].
A combined use of piezoelectric sensors and actuators is for example in aerospace engineering where a light weight of the structure, mandatory for successfully design, can cause large amplitude vibration (due to lightly damped material properties) until instability and failure; to avoid this problem piezoelectric sensors and actuators are used for vibration damping [9].
Another important role of piezoelectric is represented in noise attenuation and control [10].
The paper is organised as follows.
Differential governing equation are presented in section 2; finite element spatial discretization is briefly discussed in section 3; algorithm implementation for fluid/active-structure interaction is presented in section 4; numerical results are finally presented in section 5 and two examples are provided using piezoelectric material patches as sensors to measure structural deformations created by a fluid structure interaction.

2. GOVERNING EQUATION

In this section partial differential equation (PDE) and boundary conditions are briefly presented for solid structure, piezoelectric material and incompressible viscous fluid flow.

2-1. Solid structure

Let us consider a solid body of volume Ω_s and outward unit normal vector $\mathbf{n}$ bounded by a surface S satisfying conditions: $S = S_u \bigcup S_F$ and $S_u \bigcap S_F = 0$.

Governing equations [11] to be satisfied on Ω_s:

Dynamic equilibrium equation:

$$\tau_{ij,j} + f_i^B = \rho_s \ddot{u}_i \tag{1}$$

Strain-displacement equation:

$$\varepsilon_{ij} = \frac{1}{2}\left(u_{i,j} + u_{j,i}\right) \tag{2}$$

Constitutive equation:

$$\tau_{ij} = C_{ijhk}\varepsilon_{hk} \tag{3}$$

Essential mechanical boundary conditions (displacements) on S_u:

$$u_i = \hat{u}_i \tag{4}$$

Natural mechanical boundary conditions (forces) on S_F:

$$\tau_{ij} n_j = \hat{F}_i \tag{5}$$

Initial conditions (velocities) on Ω_s:

$$\dot{u}_i\big|_{t=0} = \hat{\dot{u}}_i\big|_{t=0} \tag{6}$$

where ρ_s is material density, u_i is the displacement vector, f_i^B the body force vector, $\hat{F}_i$ the imposed forces, ε_{ij} the strain tensor, τ_{ij} the stress tensor, C_{ijhk} the elastic constitutive tensor. Equations (1) – (6) are a set in 15 unknowns $\left(u_i, \varepsilon_{ij}, \tau_{ij}\right)$

2-2. Piezoelectric material

Let us consider a piezoelectric body of volume Ω_p and outward unit normal vector υ bounded by a surface S^p satisfying conditions: $S^p = S_u^p \bigcup S_F^p \bigcup S_Q \bigcup S_\Phi$ with $S_u^p \bigcap S_F^p = 0$ and $S_Q \bigcap S_\Phi = 0$. Governing equations [12] to be satisfied on Ω_p:

Dynamic equilibrium equation:

$$\tau_{ij,j}^p + f_i^p = \rho_p \ddot{u}_i^p \tag{7}$$

Strain-displacement equation:

$$\varepsilon_{ij}^p = \frac{1}{2}\left(u_{i,j}^p + u_{j,i}^p\right) \tag{8}$$

Constitutive coupled equation

$$\tau_{ij}^p = C_{ijhk}^p \varepsilon_{hk}^p - e_{kij} E_k \tag{9}$$

$$D_i = e_{ihk}\varepsilon_{hk}^p + \xi_{ij} E_j \tag{10}$$

Maxwell's equations for the quasi-static electric field

$$D_{i,i} = 0 \tag{11}$$

$$E_i = -\phi_{,i} \tag{12}$$

Essential mechanical boundary conditions (displacements) on S_u^p:

$$u_i^p = \hat{u}_i^p \tag{13}$$

Natural mechanical boundary conditions (forces) on S_F^p:

$$\tau_{ij}^p \upsilon_j = \hat{F}_i^p \tag{14}$$

Initial conditions (velocities) on Ω_p:

$$\dot{u}_i^p\Big|_{t=0} = \hat{\dot{u}}_i^p\Big|_{t=0} \tag{15}$$

Essential electrical boundary conditions (potentials) on S_Φ:

$$\phi = \hat{\phi} \tag{16}$$

Natural electrical boundary conditions (surface charges) on S_Q:

$$D_i \upsilon_i = \hat{Q} \tag{17}$$

where ρ_p is piezoelectric material density, u_i^p is the piezoelectric displacement vector, f_i^p the body force vector, $\hat{F}_i^p$ the imposed forces, ε_{ij}^p the strain tensor, τ_{ij}^p the stress tensor, C_{ijhk} the elastic constitutive tensor; $\hat{Q}$ the imposed charges, ϕ the electric potential, E_i the electric field vector, D_i the electric displacement vector, ξ_{ij} the dielectric permittivity tensor, e_{kij} the piezoelectric tensor. Equations (7) – (17) are a set in 22 unknowns $\left(u_i^p, \varepsilon_{ij}^p, \tau_{ij}^p, E_i, D_i, \phi\right)$

2-3. Fluid flow

Let us consider an incompressible viscous fluid in a volume Ω_f and outward unit normal vector η bounded by a surface S^f satisfying conditions: $S^f = S_v \bigcup S_T$ and $S_v \bigcap S_T = 0$.
Governing equations [13] to be satisfied on Ω_f:

Conservation of Mass

$$v_{i,i} = 0 \tag{18}$$

Conservation of Momentum

$$\rho_f\left(\dot{v}_i + v_{i,j}v_j\right) - \sigma_{ij,j} + g_i^B = 0 \tag{19}$$

Constitutive Equation

$$\sigma_{ij} = \mu_f\left(v_{i,j} + v_{j,i}\right) - p\delta_{ij} \tag{20}$$

Essential boundary conditions (velocities) on S_v:

$$v_i = \hat{v}_i \tag{21}$$

Natural boundary conditions (tractions) on S_T :

$$\sigma_{ij}\eta_j = \hat{T}_i \tag{22}$$

Initial conditions (velocities) on Ω_f :

$$v_i\big|_{t=0} = \hat{v}_i\big|_{t=0} \tag{23}$$

where ρ_f is fluid density, μ_f is dynamic fluid viscosity, p is fluid pressure, v_i is the velocity vector, g_i^B the body force vector, $\hat{T}_i$ the imposed tractions, σ_{ij} the stress tensor, δ_{ij} the Kronecker tensor.
Equations (18) – (23) are a set in 4 unknowns (v_i, p)

3. FINITE ELEMENT FORMULATION

Spatial discretization of equations (1)–(17) and boundary conditions (BC) is achieved by a classical finite element displacement formulation, instead equations (18)–(23) and relatives BC are discretized via a mixed finite element formulation in which velocity variables are mixed with force-like variable (pressure).

3-1. Active structure

Finite element model can be developed starting from a reformulation of the differential problem in a variational form (weak statement of equation field).

Finite element approximation for a solid structure is hence written, see [11] for further details:

$$[\mathbf{M}]\{\ddot{\overline{\mathbf{U}}}\} + [\mathbf{K}]\{\overline{\mathbf{U}}\} = \{\mathbf{R_B}\} + \{\mathbf{R_S}\} \tag{24}$$

$\mathbf{M}$ is the mass matrix, $\mathbf{K}$ is the stiffness matrix, $\mathbf{R_B}$ and $\mathbf{R_S}$ are the body force vector and the surface force vector respectively; $\overline{\mathbf{U}}$ is the nodal displacement vector and $\ddot{\overline{\mathbf{U}}}$ is the nodal acceleration vector.

Similarly for piezoelectric material via variational form, the finite element approximation can be derived, see [12] for further details:

$$\begin{bmatrix} \mathbf{M}_{uu}^{p} & 0 \\ 0 & 0 \end{bmatrix} \begin{Bmatrix} \ddot{\overline{\mathbf{U}}}^{p} \\ \ddot{\overline{\mathbf{\Phi}}} \end{Bmatrix} + \begin{bmatrix} \mathbf{K}_{uu}^{p} & \mathbf{K}_{u\phi}^{p} \\ \mathbf{K}_{u\phi}^{p} & \mathbf{K}_{\phi\phi}^{p} \end{bmatrix} \begin{Bmatrix} \overline{\mathbf{U}}^{p} \\ \overline{\mathbf{\Phi}} \end{Bmatrix} = \begin{Bmatrix} \mathbf{R_{BP}} \\ 0 \end{Bmatrix} + \begin{Bmatrix} \mathbf{R_{SP}} \\ 0 \end{Bmatrix} + \begin{Bmatrix} 0 \\ \mathbf{R_Q} \end{Bmatrix} \tag{25}$$

$\mathbf{M}^p$ is the mass matrix, $\mathbf{K}^p$ is the stiffness matrix, $\mathbf{R_{BP}}$ and $\mathbf{R_{SP}}$ are the body force vector and the surface force vector respectively; $\mathbf{R_Q}$ is the charge vector; $\overline{\mathbf{U}}^p$ is the nodal displacement vector and $\ddot{\overline{\mathbf{U}}}^p$ is the nodal acceleration vector, $\overline{\mathbf{\Phi}}$ is the electric potential nodal vector.

System of equations (24) and (25) are coupled together and hence a monolithic system is created and

solved for the active structure (host structure and piezoelectric material). Piezoelectric material is considered perfectly bonded to solid structure.

3-2. Fluid flow

Navier-Stokes equations must be formulated in *Arbitrary Lagrangian-Eulerian (A.L.E.)* framework [14] to describe fluid in a domain with moving boundaries.
ALE technique merges lagrangian and eulerian mesh description avoiding main drawbacks of both descriptions; the mesh nodes can be fixed as in eulerian point of view or moved as in lagrangian point of view.
Introducing the mesh velocity $\hat{v}$, the conservation of momentum equation is written in ALE formulation:

$$\rho_f \left[\dot{v}_i + v_{i,j}\left(v_j - \hat{v}_j\right)\right] - \sigma_{ij,j} + g_i^B = 0 \tag{26}$$

Finite element approximation for a incompressible fluid in ALE description is hence written, see [15] for further details:

$$\begin{bmatrix} \mathbf{M}_{vv}^f & 0 \\ 0 & 0 \end{bmatrix} \begin{Bmatrix} \dot{\overline{\mathbf{V}}} \\ \dot{\overline{\mathbf{P}}} \end{Bmatrix} + \begin{bmatrix} \mathbf{C}_{vv}^f(\mathbf{v} - \hat{\mathbf{v}}) & 0 \\ 0 & 0 \end{bmatrix} \begin{Bmatrix} \overline{\mathbf{V}} \\ \overline{\mathbf{P}} \end{Bmatrix} + \begin{bmatrix} \mathbf{K}_{vv}^f & -\mathbf{Q} \\ -\mathbf{Q}^{\mathbf{T}} & 0 \end{bmatrix} \begin{Bmatrix} \overline{\mathbf{V}} \\ \overline{\mathbf{P}} \end{Bmatrix} = \begin{Bmatrix} \mathbf{F} \\ 0 \end{Bmatrix} \tag{27}$$

$\mathbf{M}^f$ represents the mass matrix, $\mathbf{C}^f$ represents the convective transport term, $\mathbf{K}^f$ is the viscous diffusion term, $\mathbf{Q}$ is the pressure gradient term, $\mathbf{F}$ is the force vector; $\overline{\mathbf{V}}$ is the nodal velocity vector and $\overline{\mathbf{P}}$ is the nodal pressure vector.
It is important to note, for numeric analysis and implementation: $\mathbf{M}^f$ and $\mathbf{K}^f$ are symmetric matrix while $\mathbf{C}^f$ is un-symmetric, so the numerical procedure used to solve the linear system is for un-symmetric system.

3-3. Mixed velocity-pressure element

A proper combination of interpolation spaces (for velocity and pressure) is needed to avoid instabilities in the pressure field, independent of the Reynolds numbers; hence higher order is reserved to velocity shape function and lower to pressure.
The finite elements used for numerical analysis are the quadrilateral nine nodes element for the spatial discretization of the active structure and the Taylor Hood Q2-Q1 (nine nodes for the velocity / four nodes for the pressure; see fig.1) for the discretization of the fluid domain.

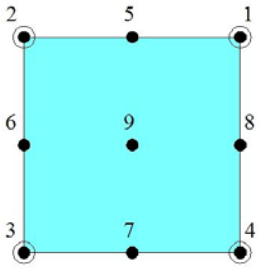

Fig. 1: Taylor Hood Q2-Q1 element

When a finite element method is formulated, some conditions such consistency, ellipticity and inf-sup condition (also know as LBB Ladyzhenskaya-Babuska-Brezzi condition) have to be verified; in this situation the finite element scheme is reliable and effective and never "fails" [11,16].
It is demonstrated the satisfaction of inf-sup condition for the Taylor Hood Q2-Q1 element [17].

4. NUMERICAL SOLUTION TECHNIQUES

4-1. Coupling algorithm

Different strategies can be used to coupling active structure (or generally structure) and fluid: strong coupling and weak coupling methods [18].
A weak coupling strategy [19] is selected in this work because it consists in solving different physics field in a staggered way; from a numerical point of view two (or more) smaller algebraic systems are assembled and solved.
Furthermore many advantages are present in partitioned formulation (vs. monolithic formulation):

- High code modularity permits an extension or modification of single physic domain keeping the others unchanged; moreover the code maintenance is easier.
- Less programming effort and previous tested and validated code can be integrated, moreover a parallelization of the code is more friendly.
- Optimized numerical techniques permit to have a less computational time effort because customized numerical algorithms can be used.

The only drawback is in a more difficult stability and generally a smaller time step Dt is required.

Weak coupling algorithm are further divided into two categories: loosey coupled (explicit) algorithms and strongly coupled (implicit) algorithms [20].
Loosey coupled algorithms are successfully used in aeroelasticty and only one solution of either field (fluid and structure) is required at each time step.
This kind of schemes are very attractive for computational efficiency, but exhibit an inherent instability for fluid-structure interaction with an incompressible fluid.
Instability can be overcome [21] using a strongly coupled (implicit) algorithm that performs iterations between fluid and structure into the same time step. Although convergence is still difficult for this schemes.
For these reasons a weak implicit coupling strategy is selected to analyse fluid interaction with an active structure.

4-2. Interface as data exchange between fluid and active structure

Interface has the role of data exchange between fluid and active structure.
Fluid applies force (due to the pressure and the shear stress) on the structure that is deformed. After deformation of the structure also the fluid domain is changed and moving boundaries must follow new structure position.
Interface is a natural or Neumann boundary condition for the structure (force imposed) and it is an essential or Dirichlet boundary condition for the fluid (velocity imposed).

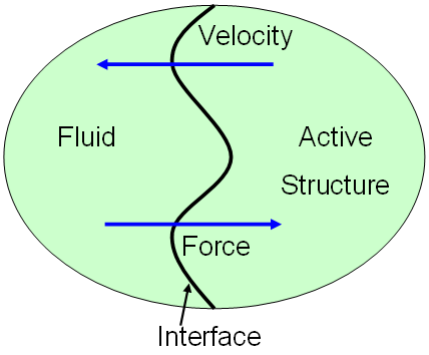

Fig. 2 Interface data exchanges between fluid and structure [Dirichlet/Neumann interaction]

This kind of interaction is the so called Dirichlet/Neumann [20].

At the interface Σ_{sf} between the solid and the fluid:

- No particles can cross it.
- Stress continuity: if a net force is applied to a surface (interface) of zero mass, the acceleration is inifinite.

Hence mathematically these conditions are imposed [2]:

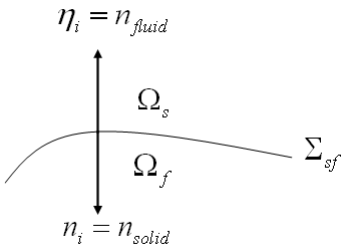

Fig. 3 Interface between fluid and active-structure

velocities: $v_i = \dot{u}_i$ (28)

forces: $\sigma_{ij}\eta_j + \tau_{ij}n_j = 0$ (29)

where τ_{ij} is the solid stress tensor, σ_{ij} is the fluid stress tensor; n_j is the solid outward normal and η_j is
the fluid outward normal; v_i is the fluid velocity and $\dot{u}_i$ is the structure velocity vector.

4-3. Mesh update

An easy mesh update algorithm is implemented, because updating of fluid mesh is required many times (every iteration) for each time step, due to structure deformations.
Mesh updating is used to avoid ill shaped elements that could cause a loss of accuracy in the solution. Algorithm used and presented in [22] is based on a smoothing procedure for mesh velocities: mesh

velocities is zero on fixed boundaries $\hat{v} = 0$ and $\hat{v} = \frac{u}{Dt}$ on moving boundaries (interface).
For all internal nodes of fluid domain, mesh velocity $\hat{v}$ is weighted according to a function of distance between the interior node and nodes on fixed and moving boundaries (e.g. an internal node near to fixed boundaries has a mesh velocity $\hat{v} \cong 0$).

4-4. Time discretization

Time marching (integration) for fluid system is a classical "alpha-family" method; equation (27) can be re-arranged in a more compact form:

$$\overline{\mathbf{M}}^f \dot{\mathbf{V}} + \overline{\mathbf{K}}^f \mathbf{V} = \overline{\mathbf{F}} \tag{30}$$

with $\overline{\mathbf{M}}^f = \begin{bmatrix} \mathbf{M}_{vv}^f & 0 \\ 0 & 0 \end{bmatrix}$; $\overline{\mathbf{K}}^f = \begin{bmatrix} \mathbf{C}_{vv}^f(\mathbf{v} - \hat{\mathbf{v}}) & 0 \\ 0 & 0 \end{bmatrix} + \begin{bmatrix} \mathbf{K}_{vv}^f & -\mathbf{Q} \\ -\mathbf{Q}^{\mathbf{T}} & 0 \end{bmatrix}$; $\mathbf{V} = \begin{Bmatrix} \overline{\mathbf{V}} \\ \overline{\mathbf{P}} \end{Bmatrix}$; $\overline{\mathbf{F}} = \begin{Bmatrix} \mathbf{F} \\ 0 \end{Bmatrix}$;

A generic "alpha-family" method [23] for the equation (30) is written:

$$\frac{1}{Dt}\overline{\mathbf{M}}^f \mathbf{V}^{n+1} + \alpha \overline{\mathbf{K}}^f \mathbf{V}^{n+1} = \frac{1}{Dt}\overline{\mathbf{M}}^f \mathbf{V}^n - (1-\alpha)\overline{\mathbf{K}}^f \mathbf{V}^n + \alpha \overline{\mathbf{F}}^{n+1} + (1-\alpha)\overline{\mathbf{F}}^n \tag{31}$$

We recommend the use of implicit method with $\alpha = 1/2$ (Crank-Nicolson) or $\alpha = 2/3$ (Galerkin).

Solid structure and piezoelectric are coupled together in a monolithic system (same matrix) and hence starting equation for transient dynamic is written (without structural damping):

$$\overline{\mathbf{M}}^a \ddot{\overline{\mathbf{U}}} + \overline{\mathbf{K}}^a \overline{\mathbf{U}} = \overline{\mathbf{F}} \tag{32}$$

with $\overline{\mathbf{U}}$ a generalized displacement vector including (solid displacement, piezoelectric displacement and electric potential); note $\overline{\mathbf{F}}$ includes external forces acting on the structures and forces transferred to the structure by the fluid along interface boundaries.
The following assumptions are used for Newmark method [11]:

$${}^{t+Dt}\dot{\overline{\mathbf{U}}} = {}^{t}\dot{\overline{\mathbf{U}}} + \left[(1-\delta)\,{}^{t}\ddot{\overline{\mathbf{U}}} + \delta\,{}^{t+Dt}\ddot{\overline{\mathbf{U}}}\right]Dt \tag{33}$$

$${}^{t+Dt}\overline{\mathbf{U}} = {}^{t}\overline{\mathbf{U}} + {}^{t}\dot{\overline{\mathbf{U}}}Dt + \left[\left(\frac{1}{2} - \alpha\right){}^{t}\ddot{\overline{\mathbf{U}}} + \alpha\,{}^{t+Dt}\ddot{\overline{\mathbf{U}}}\right]Dt^2 \tag{34}$$

Dt is the time step, $\dot{\overline{\mathbf{U}}}$ represents the velocity and $\ddot{\overline{\mathbf{U}}}$ represents the acceleration; Newmark originally proposed $\delta = 1/2$ $\alpha = 1/4$ to achieve an unconditionally stable scheme.

5. NUMERICAL RESULTS

5-1. Double clamped beam

Mass adduction of an incompressible fluid flow in a square bi-dimensional domain is simulated. Square fluid domain dimensions are: $1\,m \times 1\,m$; boundary conditions prescribed are wall condition on left, right and bottom edge, except in the central zone of the bottom edge where a traction is imposed (for a uniform pressure of 10 kPa). Upper edge constitutes interface between fluid and structure. (Figs 4a-4b)

Fluid selected is water: density $\rho = 1000\,kg/m^3$, dynamic viscosity $\mu = 1.14 \cdot 10^{-3}\,Pa \cdot s$

The walls are fixed except for the top wall that is like a double clamped beam. Beam is bended under the fluid pressure and bending deformations are revealed by piezoelectric patches bounded on the beam surface. Beam is modelled with solid bi-dimensional element under plain-strain hypothesis. Traction is imposed slowly in order to avoid beam vibrations.

Beam dimensions are: length $1m$ and thickness $0.01m$; material used is aluminium ($\rho = 2700\,kg/m^3$ $E = 80\,Gpa$ $\nu = 0.3$).

Three piezoelectric patches (length $0.1m$ and thickness $1mm$) are positioned on the beam.

Piezoelectric material properties are defined in appendix.

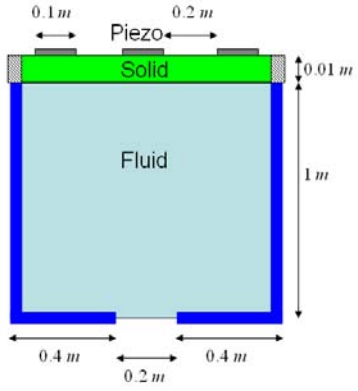

Fig. 4a Geometry

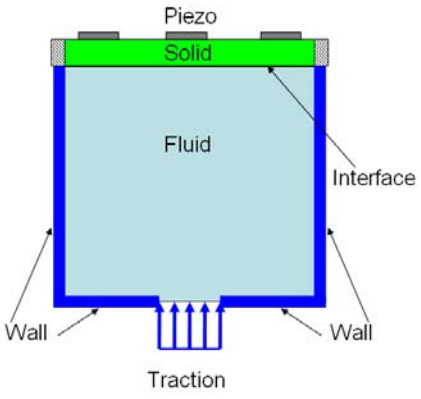

Fig. 4b Boundary condition

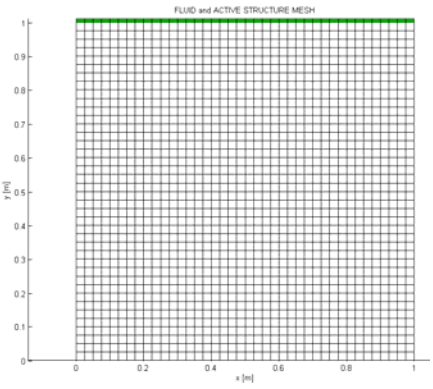

Fig. 4c Mesh used

Mesh used is constituted by 1600 Q2-Q1 elements for fluid (13122 DOF for velocity and 1681 DOF for pressure), 80 elements for solid structure (810 DOF for displacement) and 24 elements for piezoelectric material (270 DOF for displacement and 135 for electric potential). Total number of DOF for fluid active-structure interaction: 16018. (see Fig. 4c)

Results presented are: velocity magnitude (Fig. 5a), pressure field (Fig. 5b) beam transversal displacement (Fig 6) and nodal charged collected by piezoelectric sensors (Figs. 7a 7b 7c).

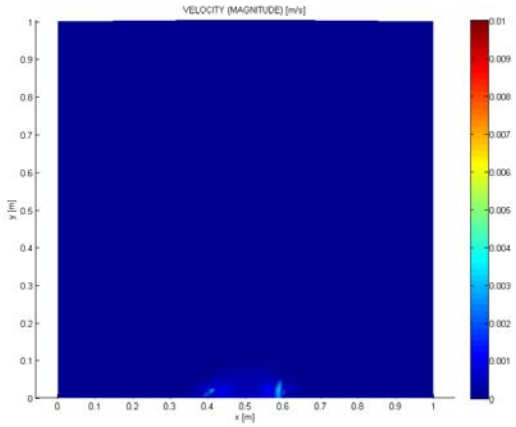

Fig. 5a: Velocity magnitude

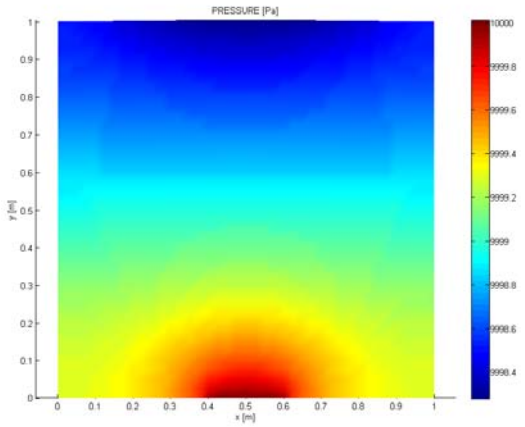

Fig. 5b: Pressure field

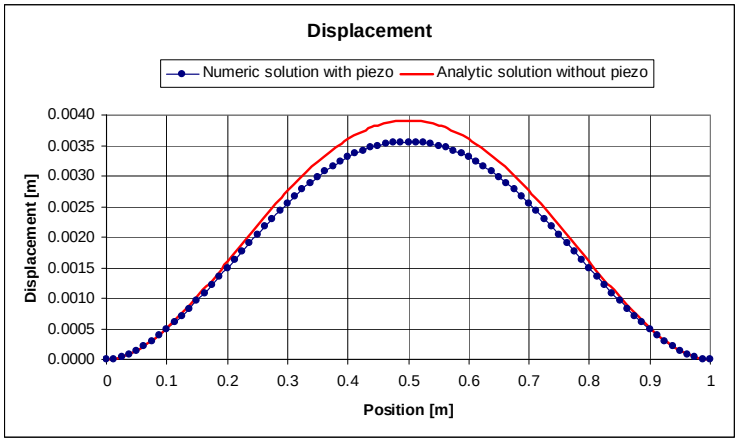

Fig. 6 Displacement: Comparison between analytic solution (no piezo) and numerical solution (with piezo)

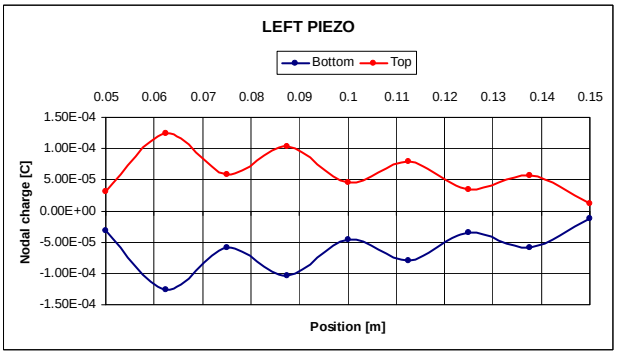

Fig. 7a Left piezoelectric sensor: nodal charge

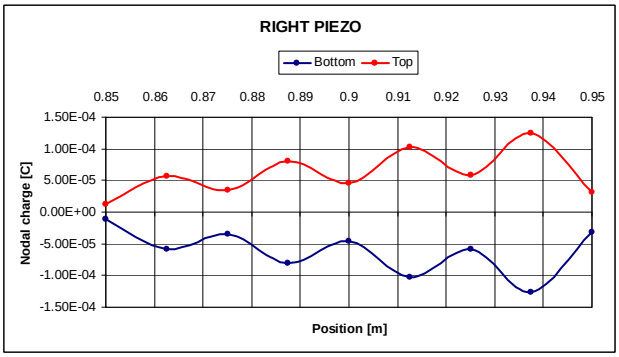

Fig. 7b Right piezoelectric sensor: nodal charge

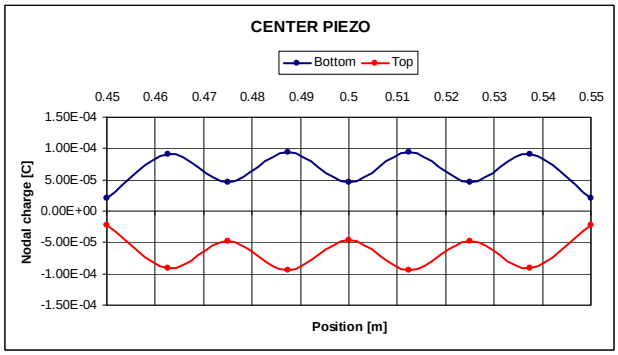

Fig. 7c Center piezoelectric sensor: nodal charge

5-2. “Balloon” structure

In this example a rectangular bi-dimensional thin structure is deformed by fluid forces acting on it; deformation is monitored by two piezoelectric sensors positioned on the left and right side of the structure

Fluid domain is $2\ m$ high and $0.4\ m$ wide; wall conditions are prescribed on the lower left and right side; traction boundary condition (for a uniform pressure of $10\ Pa$) is imposed on the bottom edge; the upper fluid domain is bounded by structure and so an interface condition is prescribed.

Fluid selected is air: density $\rho = 1.2\, kg/m^3$, dynamic viscosity $\mu = 1.83 \cdot 10^{-5} Pa \cdot s$.

Structure ($1\ m \times 0.4\ m$) with thickness $1\ mm$; structure is modelled by bi-dimensional solid element and clamped at the base on the left and right side. Material used: ($\rho = 900\, kg/m^3$ $E = 1\, Gpa$ $\nu = 0.3$).

Piezoelectric sensor are $0.2\ m$ long with a thickness of $0.5\ mm$; electrical boundary conditions prescribed for piezoelectric patches are 0 electrical potential (short circuited electrodes).

The “inflation” of the structure is followed during total time $T = 0.55\ s$ and results (snap shots) are reported for pressure field and velocity magnitude every 0.1 second.

Furthermore the nodal charged collected by piezoelectric sensors on the electrodes surface is reported.

Time step use in this analysis is $Dt = 0.01\ s$

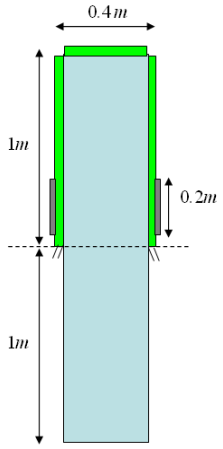

Fig. 8a: Geometry

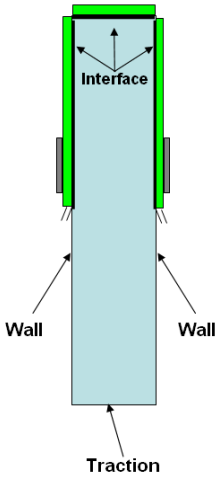

Fig. 8b: Fluid boundary condition

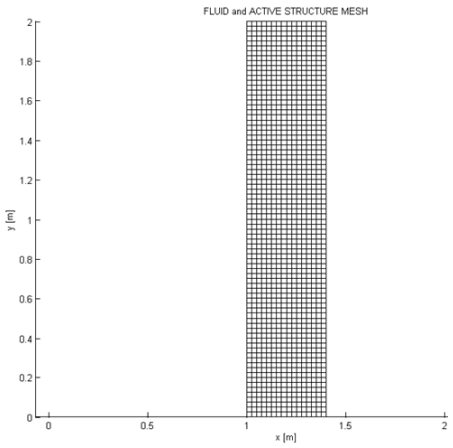

Fig. 9a: Un-deformed Mesh

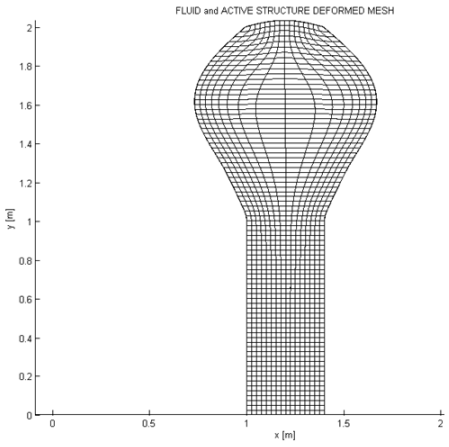

Fig. 9b: Deformed Mesh [Time 0.55 s]

Mesh used is constituted by 1280 Q2-Q1 elements for fluid (10626 DOF for velocity and 1377 DOF for pressure), 192 elements for solid structure (1946 DOF for displacement) and 32 elements for

piezoelectric material (340 DOF for displacement and 170 for electric potential).
Total number of DOF for fluid active-structure interaction: 14459.

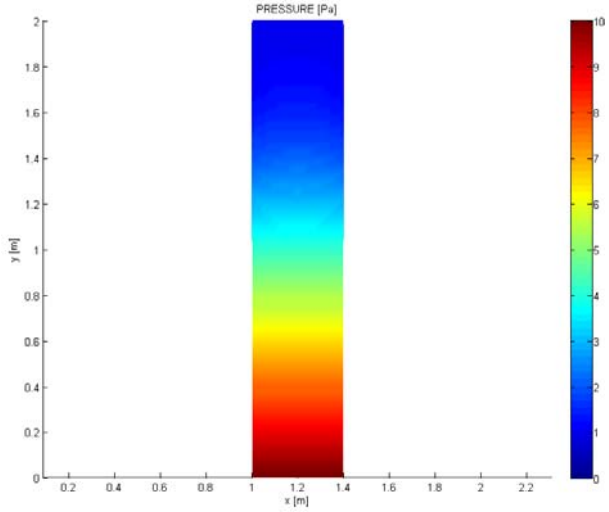

Fig. 10a: Pressure field at 0.05 s

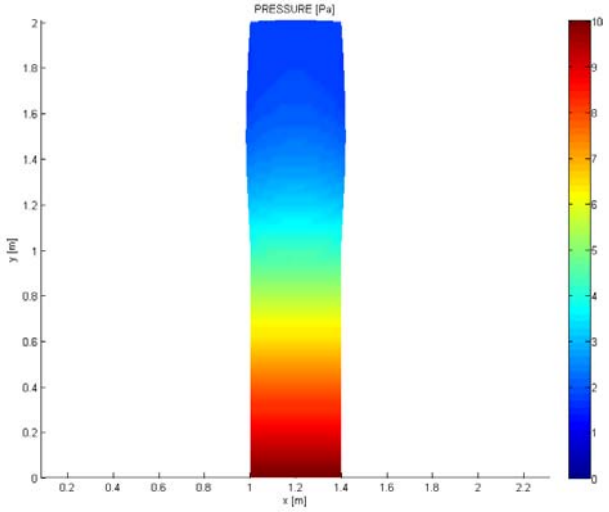

Fig. 10b: Pressure field at 0.15 s

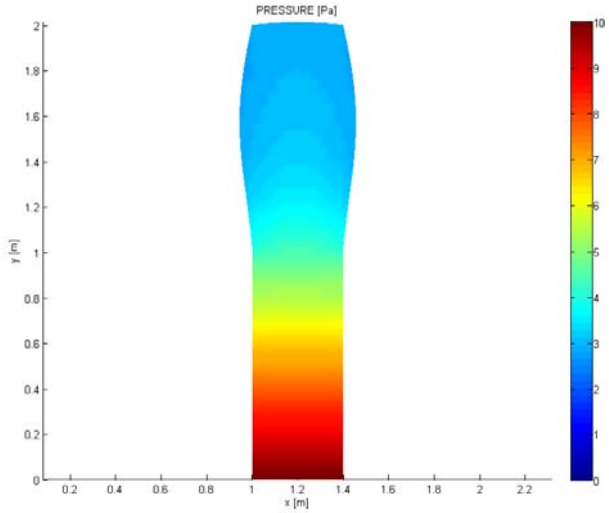

Fig. 10c: Pressure field at 0.25 s

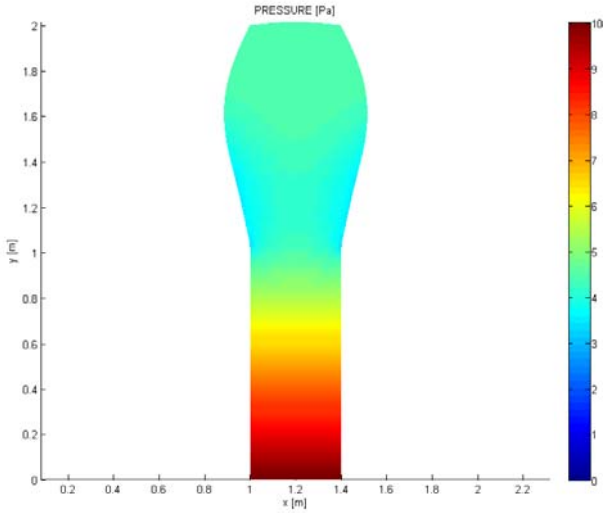

Fig. 10d: Pressure field at 0.35 s

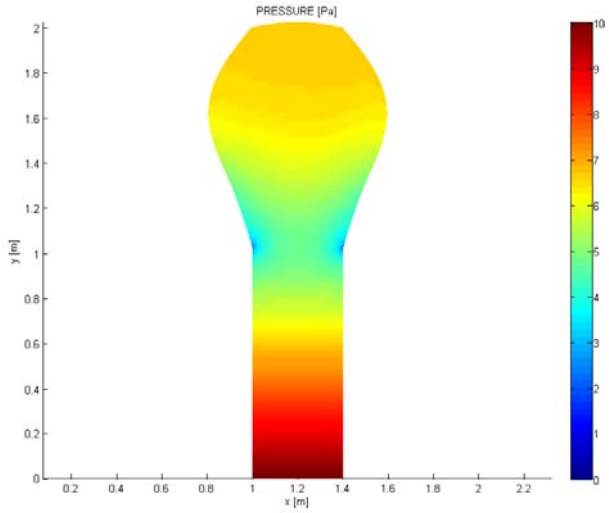

Fig. 10e: Pressure field at 0.45 s

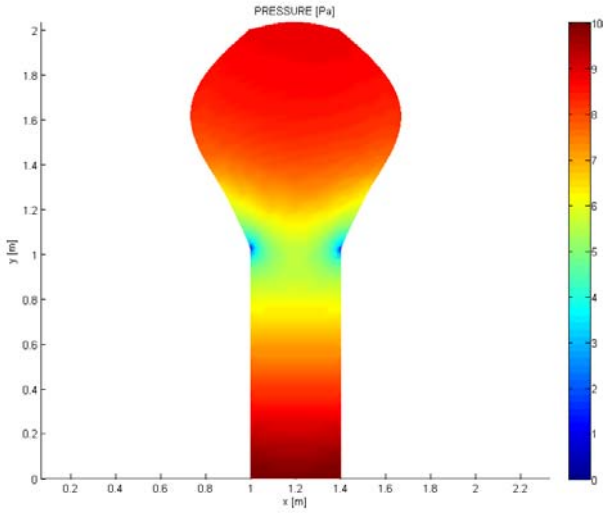

Fig. 10f: Pressure field at 0.55 s

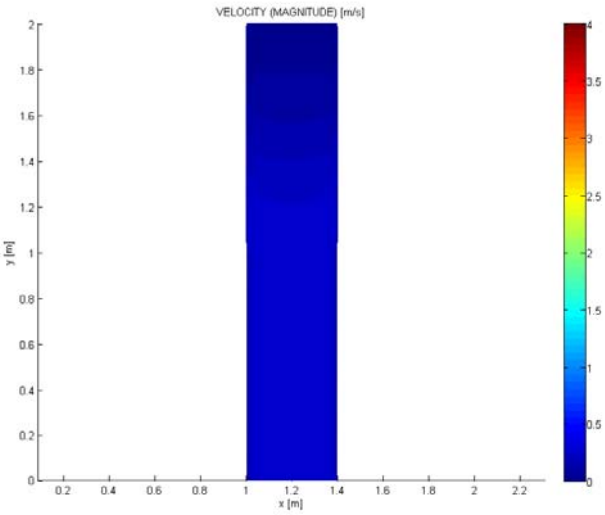

Fig. 11a: Velocity magnitude at 0.05 s

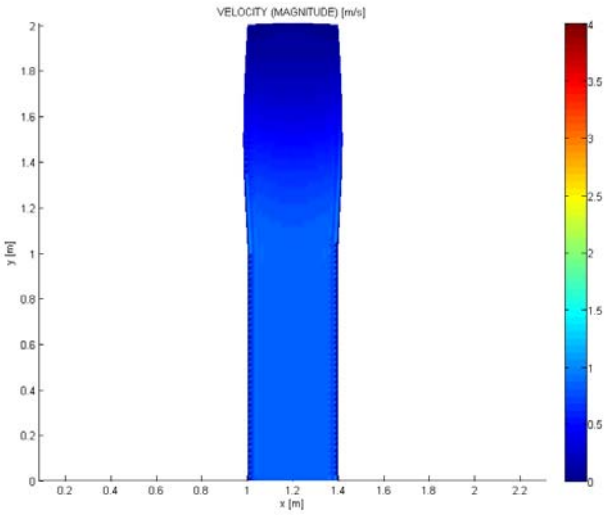

Fig. 11b: Velocity magnitude at 0.15 s

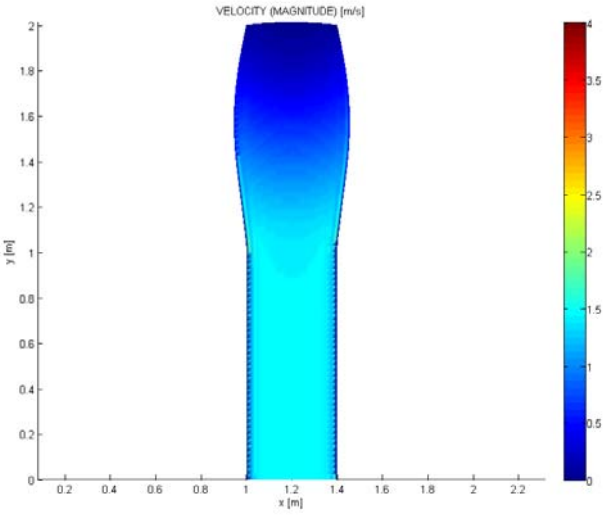

Fig. 11c: Velocity magnitude at 0.25 s

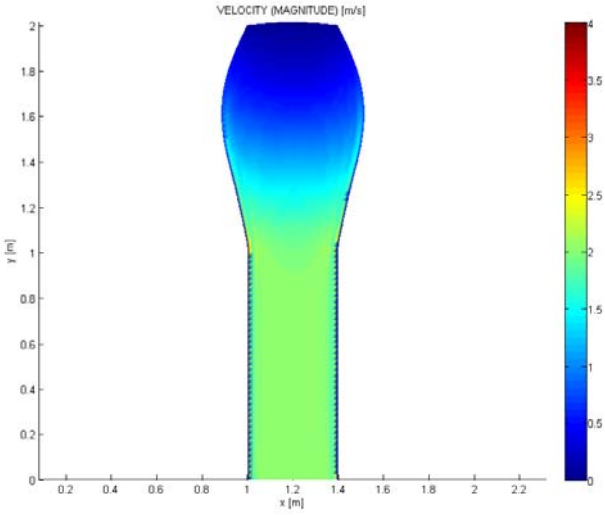

Fig. 11d: Velocity magnitude at 0.35 s

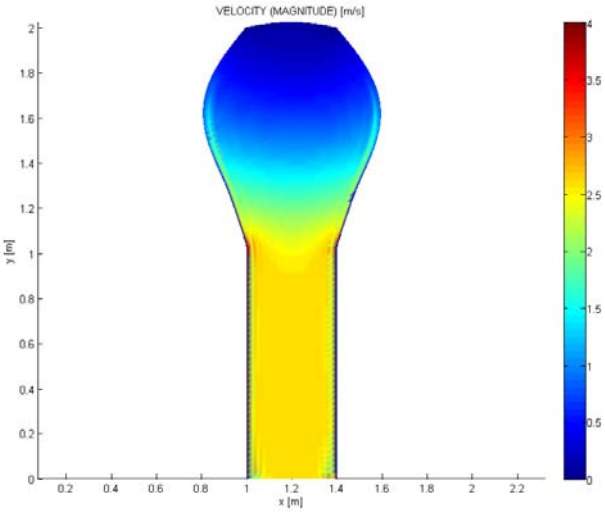

Fig. 11e: Velocity magnitude at 0.45 s

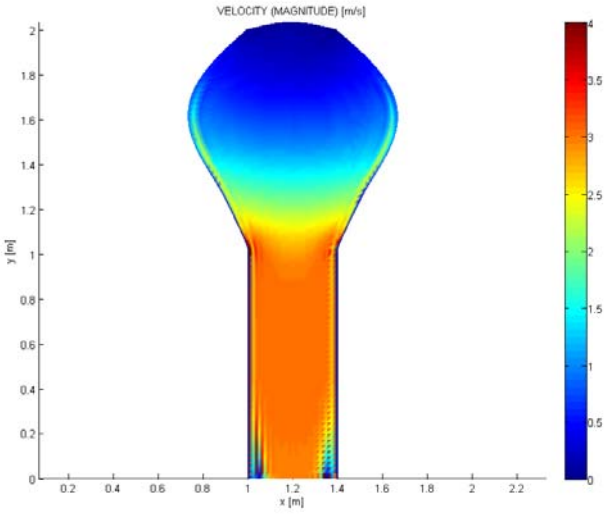

Fig. 11f: Velocity magnitude at 0.55 s

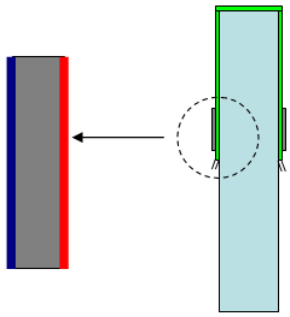

Fig. 12a: Left piezoelectric sensor

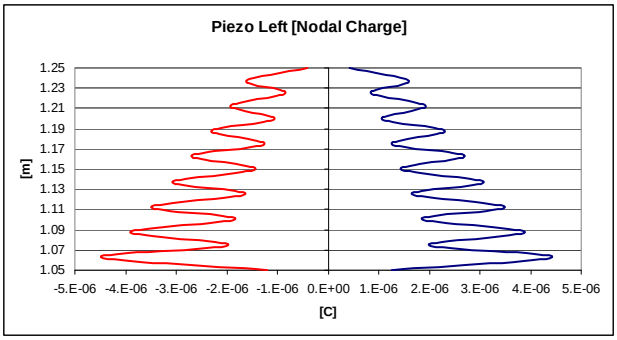

Fig. 12b: Left piezoelectric sensor (nodal charge)

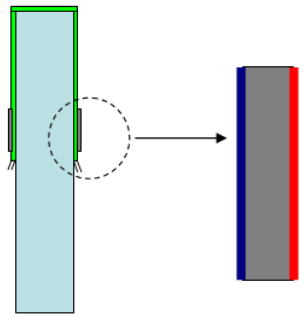

Fig. 12c: Right piezoelectric sensor

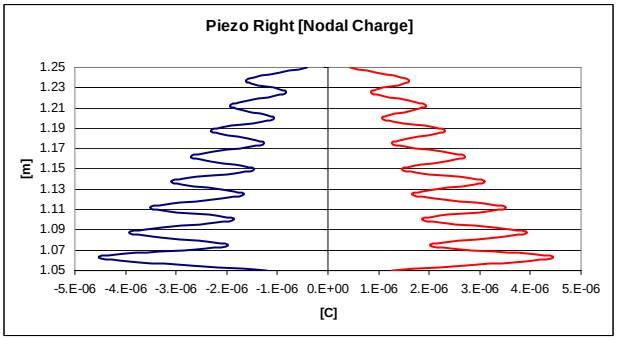

Fig. 12d: Right piezoelectric sensor (nodal charge)

6. CONCLUSIONS

A finite element model is presented to solve interactions among three different physics fields: incompressible-viscous fluid, solid structures and piezoelectric materials.
Even if the examples presented are only two-dimensional problems, the model developed is for three dimensional interactions.
First example can be interpreted as a benchmark to validate our model and numerical simulation, second example demonstrated that model presented is suitable to study important multiphysics problems such as inflatable structures.
Furthermore the potentialities of piezoelectric sensors for structural health monitoring are proven.

REFERENCES

1. Bathe, K. J., H. Zhang, and M. H. Wang, "Finite element analysis of incompressible and compressible fluid flows with free surfaces and structural interactions". *Computers and Structures*, Vol. 56, pp. 193-213 (1995).
2. Rugonyi, S., and K. J. Bathe, "On finite element analysis of fluid flows fully coupled with structural interactions". *Computational Modeling in Engineering Science* Vol. 2, pp.195-212 (2001).
3. Zallo, A., and P. Gaudenzi, "Finite element models for laminated shells with actuation capability". *Computers and Structures*, Vol. 81, pp. 1059-1069 (2003).
4. Kwak, D., C. Kiris, and C. S. Kim, "Computational challenges of viscous incompressible flows". *Computers and Fluids*, Vol. 34, pp. 283-299 (2005).
5. Preumont, A., "Mechatronics : Dynamics of Electromechanical and Piezoelectric Systems", Book, Springer (2006).
6. Mancini, S., G. Tumino, and P. Gaudenzi, "Structural health monitoring for future space vehicles".
Journal of Intelligent Material Systems and Structures, Vol. 17 (7), pp. 577-585 (2006).
7. Conway, N. J., Z. J. Traina, and S.G. Kim, "A strain amplifying piezoelectric MEMS actuator". *Journal of Micromechanics and Microengineering*, Vol. 17, pp. 781-787 (2007).
8. Cadogan, D., T. Smith, F. Uhelsky, and M. MacKusick, "Morphing Inflatable Wing Development for Compact Package Unmanned Aerial Vehicles," *Proceedings of SDM Adaptive Structures Forum* AIAA-2004-1807 (April 2004).
9. Gaudenzi, P., R. Carbonaro, and E. Benzi, "Control of beam vibrations by means of piezoelectric devices: Theory and experiments". *Composite Structures*, Vol. 50, pp. 373-379 (2000).
10. Kim, J., and B. Ko, "Optimal design of a piezoelectric smart structure for noise control". *Smart Materials and Structures*, Vol. 7, pp. 801-808 (1998).
11. Bathe, K. J., "Finite Element Procedures", Book, Prentice Hall (1996).
12. Gaudenzi, P., and K. J. Bathe, "An iterative finite element procedure for the analysis of piezoelectric continua". *Journal of Intelligent Material Systems and Structures*, Vol. 6, pp. 266-273 (March 1995).
13. Reddy, J. N., and D. K. Gartling, "The Finite Element Method in Heat Transfer and Fluid Dynamics", Book, CRC Press (2^{nd} ed.) (2002).
14. Donea, J., A. Huerta, J. Ph. Ponthot, and A. Rodriguez-Ferran "Arbitrary Lagrangian-Eulerian Methods". *Encyclopedia of Computational Mechanics*, Vol. 1 (Chapter 14) (2004).
15. Kjellgren, P., and J. Hyvarinen, "An Arbitrary Lagrangian-Eulerian finite element method". *Computational Mechanics*, Vol. 21, pp 81-90 (1998).
16. Bathe, K. J., "The inf-sup condition and its evaluation for mixed finite element methods". *Computers and Structures*, Vol. 79, pp. 243-252 (2001).
17. Gresho, P. M., and R L. Sani, "Incompressible Flow and the Finite Element Method", Book, John Wiley (1998).
18. Zhang, Q., and T. Hisada, "Studies of the strong coupling and weak coupling methods in FSI analysis". *International Journal for Numerical Methods in Engineering* Vol. 60, pp.2013-2029 (2004).
19. Felippa, C. A., K. C. Park, and C. Farhat, "Partitioned Analysis of Coupled Mechanical Systems". *Computer Methods in Applied Mechanics and Engineering*, Vol. 190, pp. 3247-3270 (2001).
20. Causin, P., J. F. Gerbeau, and F. Nobile, "Added-mass effect in the design of partitioned algorithms for fluid-structure problems". *Computer Methods in Applied Mechanics and Engineering*, Vol. 194, pp. 4506-4527 (2005).
21. Forster, C., W. A. Wall, and E. Ramm, "Artificial added-mass instabilities in sequential staggered coupling of nonlinear structures and incompressible viscous flows". *Computer Methods in Applied Mechanics and Engineering*, Vol. 196, pp. 1278-1293 (2007).
22. Teixeira, P. R. F., and A. M. Awruch, "Numerical simulation of fluid-structure interaction using

the finite element method". *Computers and Fluids*, Vol. 34, pp. 249-273 (2005).
23. Reddy, J. N., "An Introduction to Nonlinear Finite Element Analysis", Book, Oxford University Press (2004).

APPENDIX

Piezoelectric material properties (simulations use a 2D reduced model):

Piezoelectric material properties	
$C_{11} = C_{22}$	$126\ GPa$
C_{12}	$79.5\ GPa$
$C_{13} = C_{23}$	$84.1\ GPa$
C_{33}	$117\ GPa$
$C_{44} = C_{55}$	$23\ GPa$
C_{66}	$23.25\ GPa$
Density	$7730\ kg/m^3$
$e_{31} = e_{32}$	$-6.5\ C/m^2$
e_{33}	$23.3\ C/m^2$
$e_{24} = e_{15}$	$17\ C/m^2$
$\xi_{11} = \xi_{22}$	$13\ nF/m$
ξ_{33}	$15.03\ nF/m$

Table 1: Piezoelectric material properties